AD-A031 716 MASSACHUSETTS INST OF TECH LEXINGTON LINCOLN LAB F/G 20/1
PROGRAMMABLE MATCHED FILTERING WITH ACOUSTO-ELECTRIC CONVOLVERS--ETC(U)
SEP 75 J H CAFARELLA, W M BROWN, J A ALUSOW
UNCLASSIFIED MS-4098 ESD-TR-76-264 NL

1 OF 1
AD
A031716

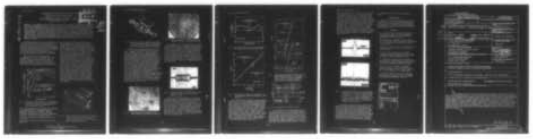

END

DATE
FILMED
12-76

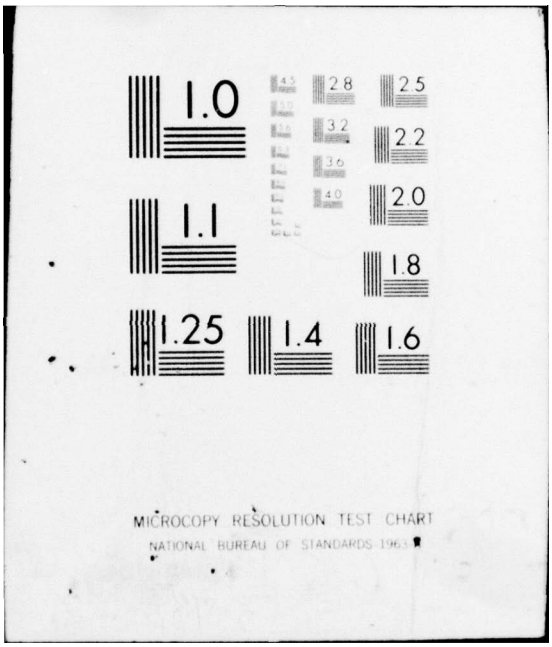
1.0
1.1
1.25
1.4
1.6
1.8
2.0
2.2
2.5
2.8
3.2
3.6
4.0
MICROCOPY RESOLUTION TEST CHART
NATIONAL BUREAU OF STANDARDS-1963

PROGRAMMABLE MATCHED FILTERING WITH ACOUSTOELECTRIC CONVOLVERS IN SPREAD-SPECTRUM SYSTEMS*

J. H. Cafarella, J. A. Alusow, W. M. Brown, E. Stern
Lincoln Laboratory, Massachusetts Institute of Technology
Lexington, Massachusetts 02173

ABSTRACT: Acoustoelectric convolvers for a spread-spectrum communication application are described with a 100-MHz-bandwidth capability. The use of convolvers as programmable matched filters provides the ability to change the coding waveform from bit-to-bit, thus offering improved multipath performance, security against decoding, and protection against repeat jamming. In this paper we describe design and performance details of a prototype convolver which processes signals of 10 μs duration with a 100-MHz bandwidth. A dynamic range of 50 dB is obtained and error signals are 30 dB below the output signal with input signal levels of +14 dBm. A test circuit is described which creates typical spread-spectrum signals in which each bit is encoded into 512 chips and data is encoded by inverting the phase of an entire bit at a data rate of 100 kbits/s. Examples of typical convolver outputs will be described, including spurious artifacts due to a pseudorandom-shift-register code, with a code-cycle time of 36 minutes.

Acoustoelectric convolvers have been studied at our laboratory and elsewhere[1,2,3] for several years and the results of these studies have been incorporated in a convolver design to operate at an input center frequency of 300 MHz, a bandwidth of 100 MHz, and a time-bandwidth product of 1000. The device was optimized for a spread-spectrum application in which drive power is of critical importance, and a 40 dB dynamic range was specified with maximum input power levels of +10 dBm.

The figure of merit F of these devices[4] is defined by $F=10 \log (P_3/P_1P_2)$, where P_1 and P_2 are input powers and P_3 is the output power level. The quantity F is plotted in Fig. 1 as a function of gap distance between a silicon strip and lithium-niobate surface for 3 values of silicon resistivity. This calculation included the transfer characteristics

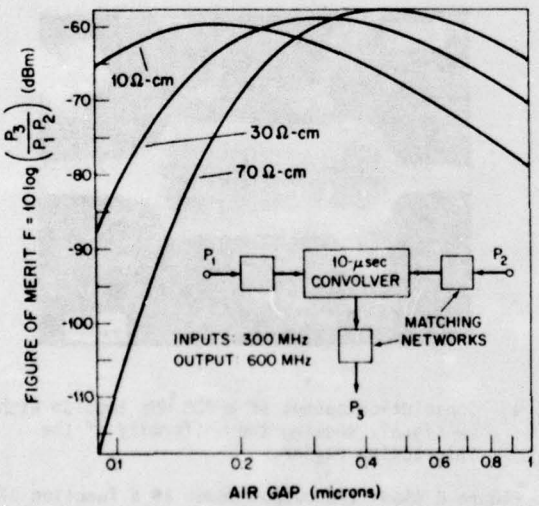

Fig. 1 Theoretical figure-of-merit vs. gap dimensions for three silicon resistivities. The calculation includes transfer characteristics of input and output circuitry.

of the input impedance-matching networks and transducers, and the output networks. The impedance-inverter networks at the inputs are designed to optimize the transfer characteristics of 2.5-period input transducers with an acoustic aperture of 50 wavelengths at 300 MHz. The nonlinear interaction region is 3.84 cm long, which corresponds very nearly to a half wavelength of electromagnetic energy in lithium niobate at the output center-frequency of 600 MHz. The 0.75-mm-wide silicon strip acts as a center conductor of a microstrip transmission line with a 30-ohm characteristic impedance. The ground planes, which are on the top surface of the lithium niobate, are 1.5 mm apart. In order to avoid long-line effects,[5] the ends of the silicon strip are connected to impedance terminations. The nonlinear-interaction calculation is based on previously published work[6]. In Fig. 1 notice that 10-ohm-cm silicon provides a relatively constant figure of merit of approximately 60 dB over a gap distance ranging from 0.15μm to 0.22μm. Also notice that a 30-ohm-cm resistivity gives approximately the same figure of merit for gaps ranging from 0.2μm to 0.4μm. Consequently, a resistivity of 15 ohm-cm and a gap of 0.2μm provides a design which is forgiving to variations in resistivity and gap dimensions, providing stray electrostatic fields, surface contaminants, or variations in surface-trap densities do not distort the carrier distribution at the silicon interface. We have found that the removal of a 0.2μm-thick thermal oxide hydrofluoric acid just prior to assembly creates a depleted silicon surface which appears to be impervious to stray electrostatic fields and to contaminants.

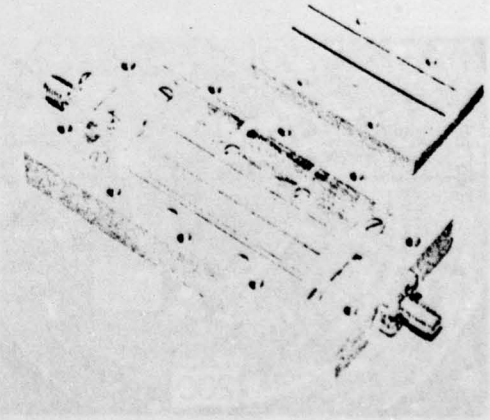

Fig. 2a $LiNbO_3$ substrate and silicon strip. The $LiNbO_3$ surface is coated with aluminum transducer and ground-plane patterns, and contains .3μm spacer posts between ground planes. The silicon strip is located on RTV gel.

*This work was sponsored by the Advanced Research Projects Agency.

1975 Ultrasonics Symposium Proceedings, IEEE Cat. #75 CHO 994-4SU

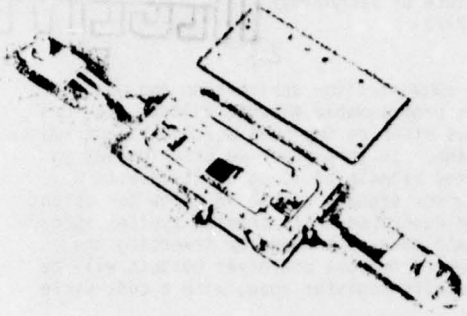

Fig. 2b Assembled convolver. Output transformer is in the middle and terminations are at ends of inner block. Input impedance-inverter networks are connected to two input terminals.

Figure 2a shows the component parts of the convolver. The silicon strip with three 10-mil gold leads is embedded in RTV gel. These wires pass through insulated holes in the interior brass block. The lithium- niobate surface has deposited on it aluminum transducers, ground planes and shields. The region between the ground planes contains a pseudo-random distribution of 0.3-μm-high spacer posts[7]. The silicon is positioned over the spacer posts and the interior brass block is clamped to the outer block with screws. This compresses the RTV gel around the silicon, and holds it in place against the spacer posts. The impedence termination in the cavities at the ends of the inner block consists of a 30-ohm resistance in series with a capacitive reactance of 10 ohms, which compensates for the inductance in the wires. The center wire is connected to a 4-to-1 impedance transformer which provides an output impedance of approximately 60 ohms. The input-impedance-inverter cables and transformers are visible in Fig. 2b. A plot of the input and output impedances as a function of frequency are shown in Fig. 3. The plots follow almost constant Γ circles on the Smith chart with a VSWR of less than 3 on all ports.

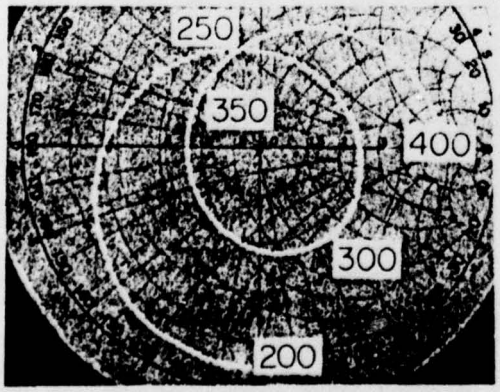

Fig. 3a Input impedance of assembled convolver. Operating bandwidth is from 250 to 350 MHz.

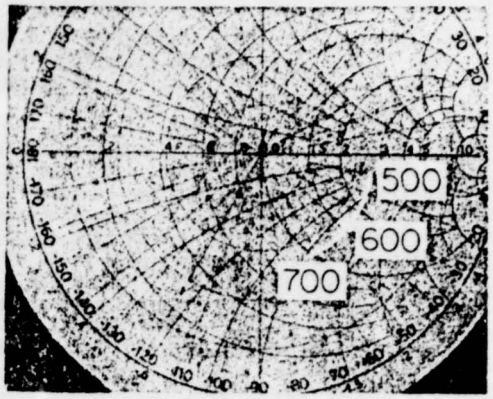

Fig. 3b Output impedance of assembled convolver. Operating bandwidth is from 500 to 700 MHz.

The convolution of a short impulse with a long CW pulse is shown in Fig. 4. The short impulse scans the strength of the convolution process as a function of position in the convolver. Notice that the amplitude fluctuates by less than 1/2 dB. The quality factor F of the convolver as a function of frequency for CW pulses is shown in Fig. 5. In this device, a 10-ohm-cm silicon strip and a gap of 0.3μm was used. Also note that 1-dB bandwidth of 100 MHz is available in the device and that the quality factor is only 3 dB below the predicted value in Fig. 1. This discrepency is mostly due to ohmic losses in the impedance transformers and diffraction.

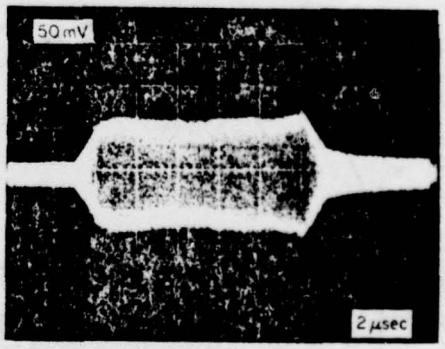

Fig. 4 Convolution output of a 300 MHz impulse with a CW signal, showing the uniformity of the interaction region.

Figure 6 shows the output power as a function of input power levels. In this instance,the output power in dBm is plotted as a function of the sum of the logs of the two input levels. Note that the output is linear with input power up to input power levels of +14 dBm, at which point, 1-dB gain compression is obtained. The output bandwidth of 200 MHz together with an amplifier noise figure of 3 dB establishes an output noise level of -88 dBm. The output power at the 1-dB-compression point is -38 dBm. Consequently, a dynamic range of 50 dB is available. If the inputs are reduced to +10 dBm, a dynamic range of 40 dB is obtained, which agrees with the design goals.

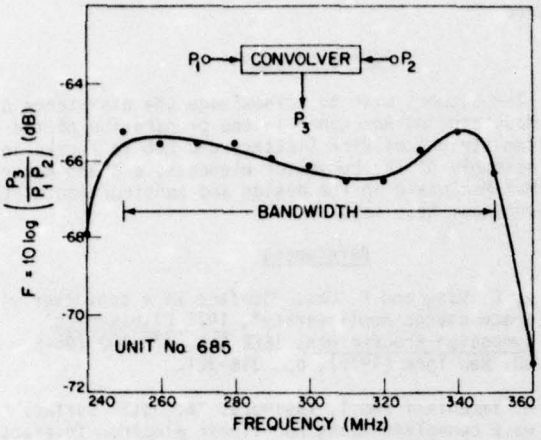

Fig. 5 Measured figure of merit vs. input frequency. This 1 dB bandwidth is greater than 100 MHz.

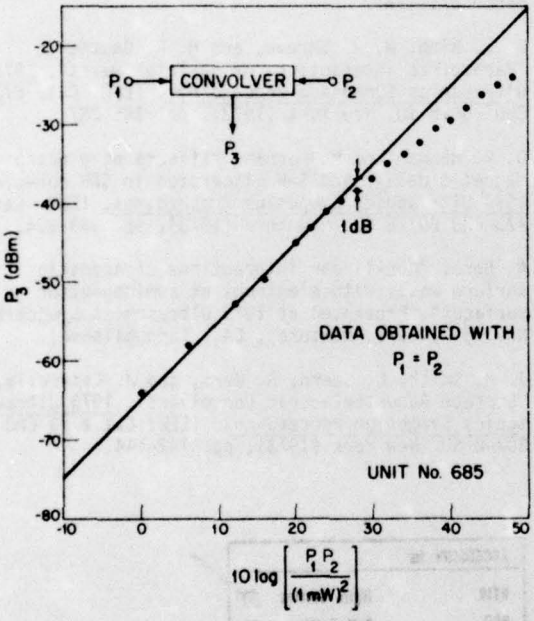

Fig. 6 Output power vs. product of input powers. The two input powers are maintained equal as they are varied.

The principal spurious signal in the convolver was found to be due to the self-convolution of the reference signal, which is reflected from the transducer at the opposite end of the crystal, and convolves with itself. If the reference is a CW signal, the reflected signal correlates with the direct signal and a maximum output signal is obtained which is plotted in Fig. 7. Notice that if the input power level is +10 dBm, this self-convolution signal is -70 dBm. However if the reference signal is coded with a wide-band pseudo-random code, coherent correlation does not take place, and the signal is 20 dB below the CW output level. Thus, a coded-input-reference power level of +10 dBm produces, in this device, a spurious signal of -90 dBm, which is below the thermal noise at the output.

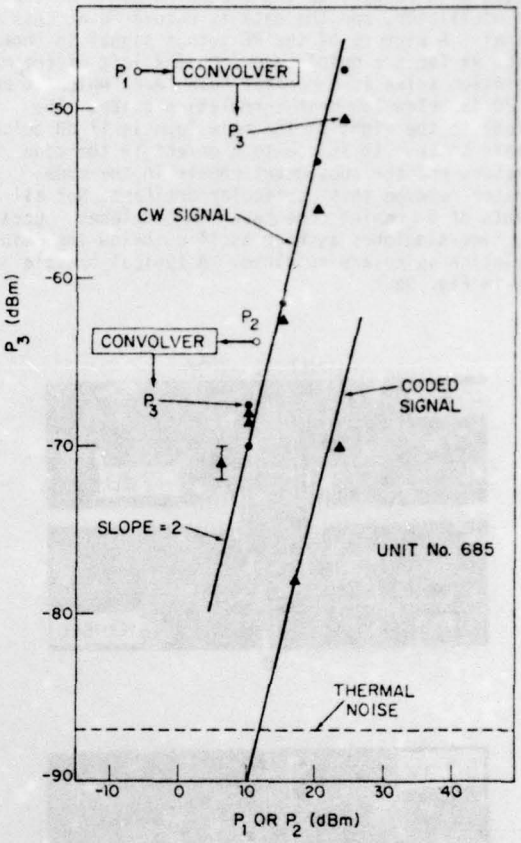

Fig. 7 Autoconvolution output of CW and pseudorandom phase-shift-keyed signals vs. input power level, when only one input is connected. This signal arises as a result of partial reflection from the opposite transducer.

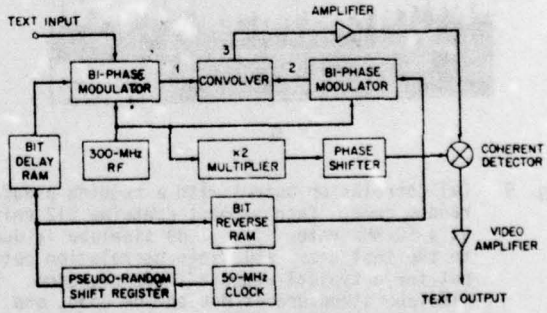

Fig. 8 Block diagram of convolver test set.

A block diagram of the acoustoelectric-convolver test set is shown in Fig. 8. A 50-MHz clock drives a pseudo-random shift register which creates a code with a cycle-time of 36 minutes. 512-bit sections of the code are loaded into the delay and bit-reverse random-access memories (RAM). The stored signal is read out in reverse order from the reverse RAM. The outputs of these components modulate 300-MHz RF carriers and are connected to the convolver input terminals. The input

data causes either a 0 or π phase shift of the carrier. The output of the convolver is amplified and phase-detected with respect to the second harmonic of the local oscillator, and the data is recovered at this terminal. A picture of the RF output signal is shown in Fig. 9a for a running code. On the left of the main correlation spike is a general hash level which is more than 20 dB below the main correlation spike. The sidelobe to the right of the main lobe is 17 dB below the main spike. It is due to a defect in the code generator, and the subsequent repair in the code generator removed this particular artifact. Not all segments of a running code have low sidelobes. Occasionally, time-sidelobes as high as 14 dB below the main correlation spike are obtained. A typical example is shown in Fig. 9b.

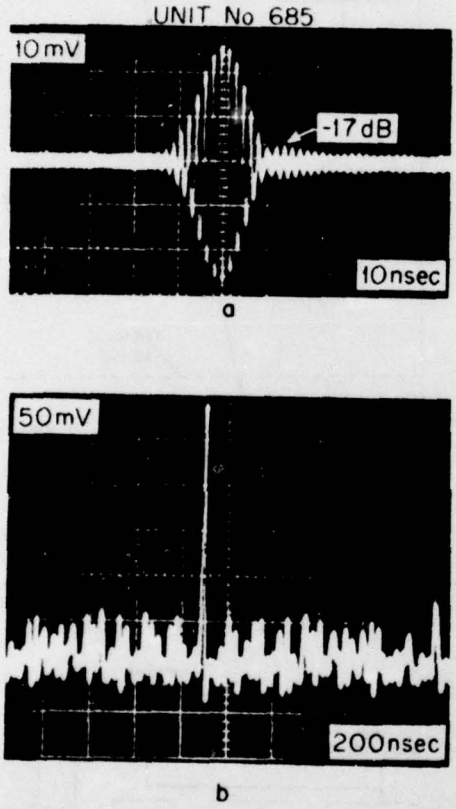

Fig. 9 (a) Correlation output with a running pseudo-random code. Each segment contains 512 chips at a 50-MHz rate. The 17 dB sidelobe is due to the test set. (b) Video correlation output for a typical repeated code sequence. The sidelobe structure is due to the code, and contains spurious sidelobes as high as 14 dB below the correlation peak.

In conclusion, an acoustoelectric convolver has been designed which provides a maximum dynamic range of 50 dB, and a 40-dB dynamic range when input power levels are limited to +10 dBm. The device has a bandwidth of 100 MHz and time-bandwidth product of 1000. It has been used for decoding continuously changing pseudorandom code sequences for spread-spectrum systems. The technology for fabricating these devices has been perfected to the point where 3 out of 4 devices have had identical electrical characteristics. Spurious signals are well below the sidelobe level associated with spread-spectrum codes, and can therefore be ignored.

Acknowledgements

The authors wish to acknowledge the assistance of Bob Mountain and Ron Cohen in the preparation of the silicon strips, of Rick Slattery and Bob Konieczka in the assembly of the convolver elements, and Bob Baker and Mal MacDonald in the design and construction of the pseudorandom test sets.

References

1. W. C. Wang and P. Das, "Surface wave convolver via space charge nonlinearity", 1972 Ultrasonics Symposium Proceedings, IEEE Cat. #72 CHO 708-8 SU, New York (1972), pp. 316-321.

2. M. Yamanishi and T. Kawamura, "Acoustic surface wave convolver using non-linear electron interactions in coupled semiconductor-piezoelectric systems", ibid pp. 288-291.

3. J. M. Smith, E. Stern, A. Bers, "Accumulation-layer surface wave convolver", Elect. Lett. 9, No. 6, March 22, 1973.

4. G. S. Kino, W. R. Shreve, and H. R. Gautier, "Parametric interactions of Rayleigh waves", 1972 Ultrasonics Symposium Proceedings, IEEE: Cat. #72 CHO 708-8 SU, New York (1972), pp. 285-287.

5. D. P. Morgan and M. Hannah, "Effects of electromagnetic delays and SAW dispersion in SAW convolvers", 1974 Ultrasonics Symposium Proceedings, IEEE: Cat. #73 CHO 807-8 SU, New York (1973), pp. 333-334.

6. A. Bers, "Non-linear interactions of acoustic surface waves with electrons at semiconductor surfaces", Presented at 1973 Ultrasonics Symposium, Nov. 5-7, 1973, Monterey, CA., (unpublished).

7. J. M. Smith, E. Stern, A. Bers, and J. Cafarella, "Surface Acoustoelectric Convolvers", 1973 Ultrasonics Symposium Proceedings, IEEE: Cat.# 73 CHO 807-8 SU, New York (1973), pp. 142-144.

UNCLASSIFIED

SECURITY CLASSIFICATION OF THIS PAGE (When Data Entered)

REPORT DOCUMENTATION PAGE	READ INSTRUCTIONS BEFORE COMPLETING FORM
1. REPORT NUMBER (18) ESD-TR-76-264 (19)	2. GOVT ACCESSION NO. / 3. RECIPIENT'S CATALOG NUMBER
4. TITLE (and Subtitle) (6) Programmable Matched Filtering with Acousto-electric Convolvers in Spread-Spectrum Systems	5. TYPE OF REPORT & PERIOD COVERED (9) Journal Article
	6. PERFORMING ORG. REPORT NUMBER (14) MS-4098
7. AUTHOR(s) (10) John H. Cafarella, ~~John H.~~ ~~Alusow~~, John A. Alusow; William M. Brown, ~~William M.~~ ~~Stern~~, Ernest Stern	8. CONTRACT OR GRANT NUMBER(s) F19628-73-C-0002
9. PERFORMING ORGANIZATION NAME AND ADDRESS Lincoln Laboratory, M.I.T. P.O. Box 73 Lexington, MA 02173	10. PROGRAM ELEMENT, PROJECT, TASK AREA & WORK UNIT NUMBERS ARPA 600
11. CONTROLLING OFFICE NAME AND ADDRESS Advanced Research Projects Agency 1400 Wilson Boulevard Arlington, VA 22209	12. REPORT DATE (11) 22 September 1975
	13. NUMBER OF PAGES 4 (12) 5 p.
14. MONITORING AGENCY NAME & ADDRESS (if different from Controlling Office) Electronic Systems Division Hanscom Air Force Base Bedford, MA 01730	15. SECURITY CLASS. (of this report) UNCLASSIFIED
	15a. DECLASSIFICATION DOWNGRADING SCHEDULE n/a

16. DISTRIBUTION STATEMENT (of this Report)

Approved for public release; distribution unlimited.

17. DISTRIBUTION STATEMENT (of the abstract entered in Block 20, if different from Report)

18. SUPPLEMENTARY NOTES

1975 Ultrasonics Symposium Proceedings, IEEE Cat. #75, CHO 994-4SU

19. KEY WORDS (Continue on reverse side if necessary and identify by block number)

Spread-spectrum communication
Programmable matched filtering
Acoustoelectric convolvers

20. ABSTRACT (Continue on reverse side if necessary and identify by block number)

Acoustoelectric convolvers for a spread-spectrum communication application are described with a 100-MHz-bandwidth capability. The use of convolvers as programmable matched filters provides the ability to change the coding waveform from bit-to-bit, thus offering improved multipath performance, security against decoding, and protection against repeat jamming. In this paper we describe design and performance details of a prototype convolver which processes signals of 10 μs duration with a 100-MHz bandwidth. A dynamic range of 50 dB is obtained and error signals are 30 dB below the output signal with input signal levels of +14 dBm. A test circuit is described which creates typical spread-spectrum signals in which each bit is encoded into 512 chips and data is encoded by inverting the phase of an entire bit at a data rate of 100 kbits/s. Examples of typical convolver outputs will be described, including spurious artifacts due to a pseudorandom-shift-register code, with a code-cycle time of 36 minutes.

207 650

DD FORM 1 JAN 73 1473 EDITION OF 1 NOV 65 IS OBSOLETE

UNCLASSIFIED

SECURITY CLASSIFICATION OF THIS PAGE (When Data Entered)